

Supporting Information for:

Synthesis and characterization of a series of nickel(II) alkoxide precursors and their utility for
Ni(0) nanoparticle production

by

LaRico J. Treadwell, Timothy J. Boyle* Marie V. Parkes,

Adam Phelan,^a David P. Young,^a

List of Supporting Figures

Figure S1. Structure plot of **2**. Thermal ellipsoids of heavy atoms drawn at the 30% level and carbon atoms represented by ball and stick diagrams for clarity.

Figure S2. Structure plot of **3**. Thermal ellipsoids of heavy atoms drawn at the 30% level and carbon atoms represented by ball and stick diagrams for clarity.

Figure S3. UV-vis spectra for **2** (◆ calculated singlet; = x calculated triplet, ■ experimental).

Figure S4. UV-vis spectra for **3** (◆ calculated singlet; = x calculated triplet, ■ experimental).

Figure S5. UV-vis spectra for **4** (◆ calculated singlet; = x calculated triplet, ■ experimental).

Figure S6. UV-vis spectra for **5** (◆ calculated singlet; = x calculated triplet, ■ experimental).

Figure S7. UV-vis spectra for **6** (◆ calculated singlet; = x calculated triplet, ■ experimental).

Figure S8. TGA analysis of **1** taken at 25 – 550 °C at a rate of 5 °C per minute under flowing argon.

Figure S9. TGA analysis of **6** taken at 25 – 550 °C at a rate of 5 °C per minute under flowing argon.

Figure S10. PXRD for the resultant materials from TGA analysis of **1** taken at a range of 10 - 90° with a scan rate of 0.15 °/sec.

Figure S11. PXRD for the resultant materials from TGA analysis of **6** taken at a range of 10 - 90° with a scan rate of 0.15 °/sec.

Figure S12. FTIR spectral data (shown from 3800 to 2400 cm^{-1}) for the resultant nanoparticles from **1** and **6**.

Figure S1. Stick representation of the structure of $\text{Ni}(\text{L})_2$ showing the displacement ellipsoids at the 50% probability level. The carbon atoms are shown as spheres of arbitrary radii.

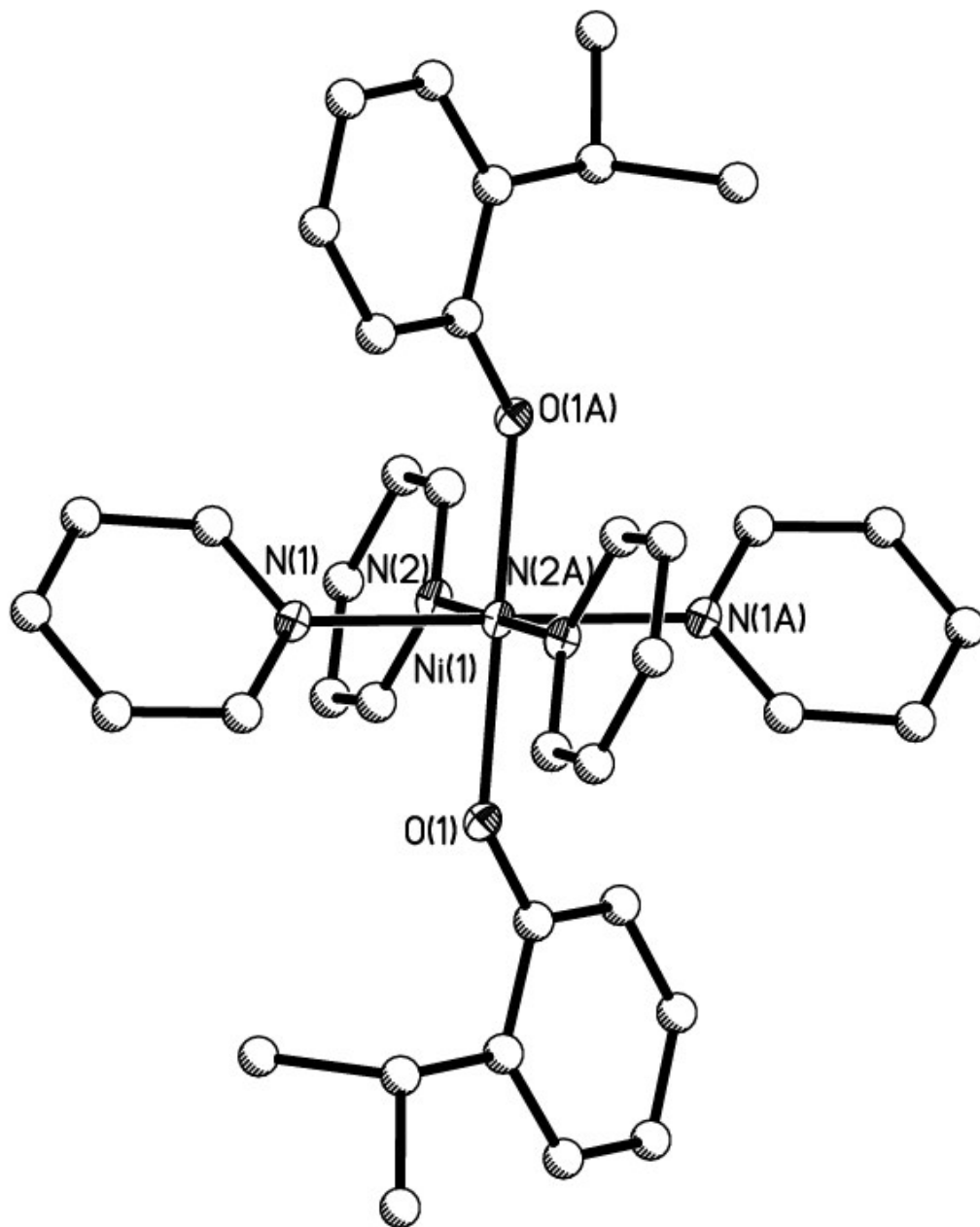


Figure S2. Structure plot of **3**. Thermal ellipsoids of heavy atoms drawn at the 30% level and carbon atoms represented by ball and stick diagrams for clarity.

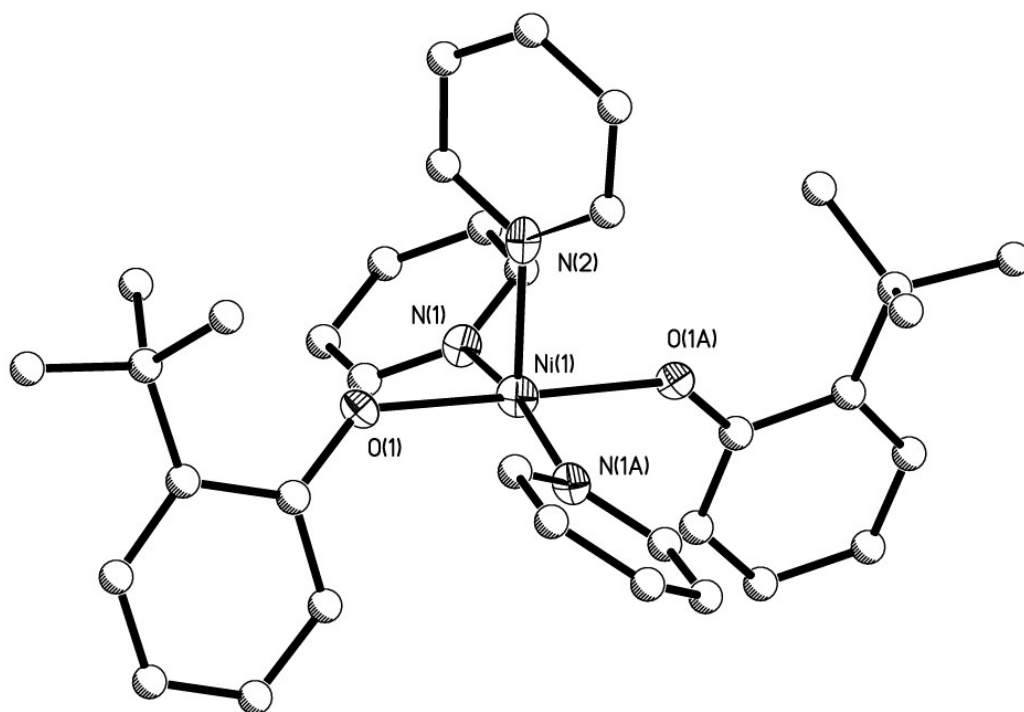


Figure S3. UV-vis spectra for **2** (◆ calculated singlet; × calculated triplet, ■ experimental).

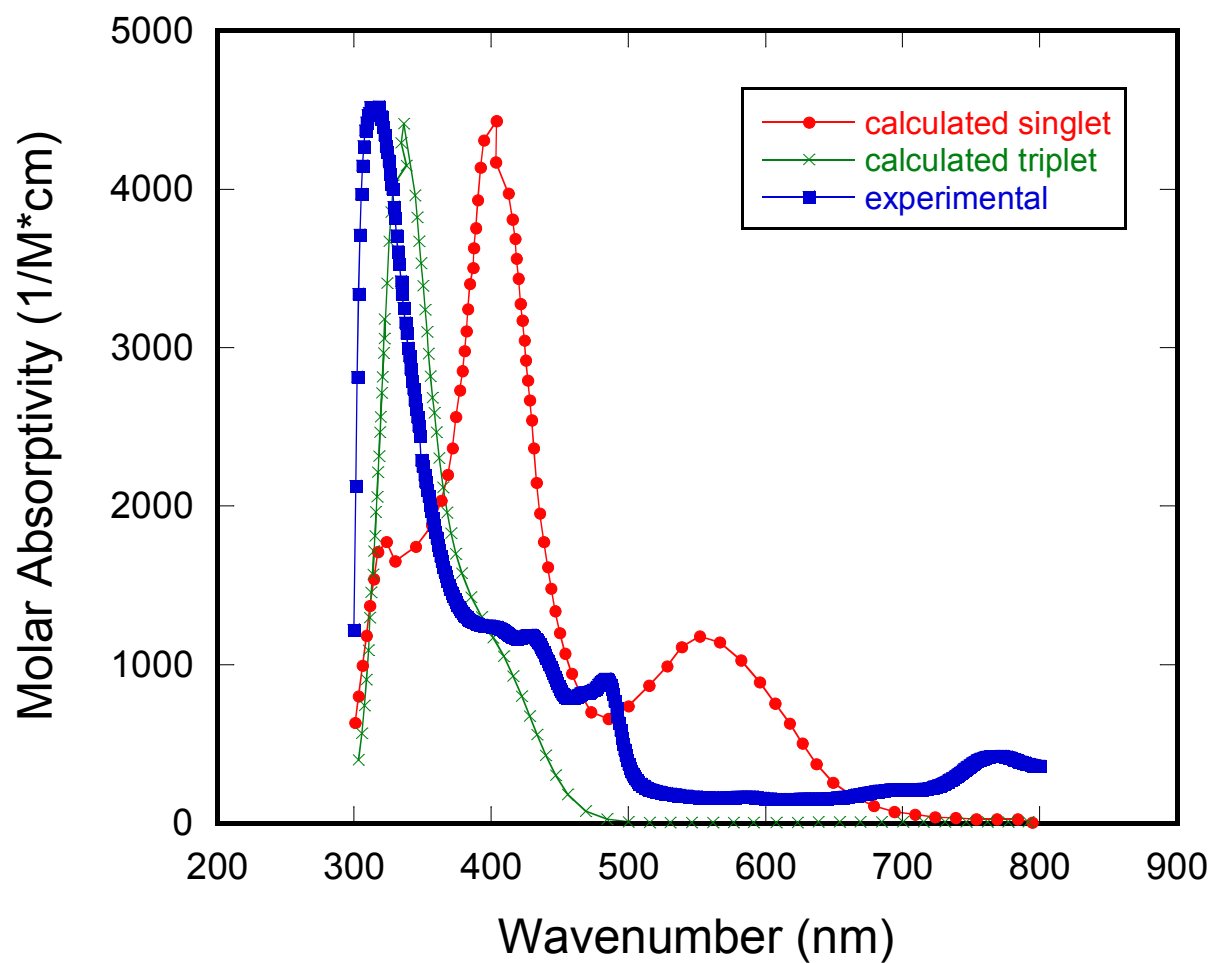


Figure S4. UV-vis spectra for **3** (◆ calculated singlet; × calculated triplet, ■ experimental).

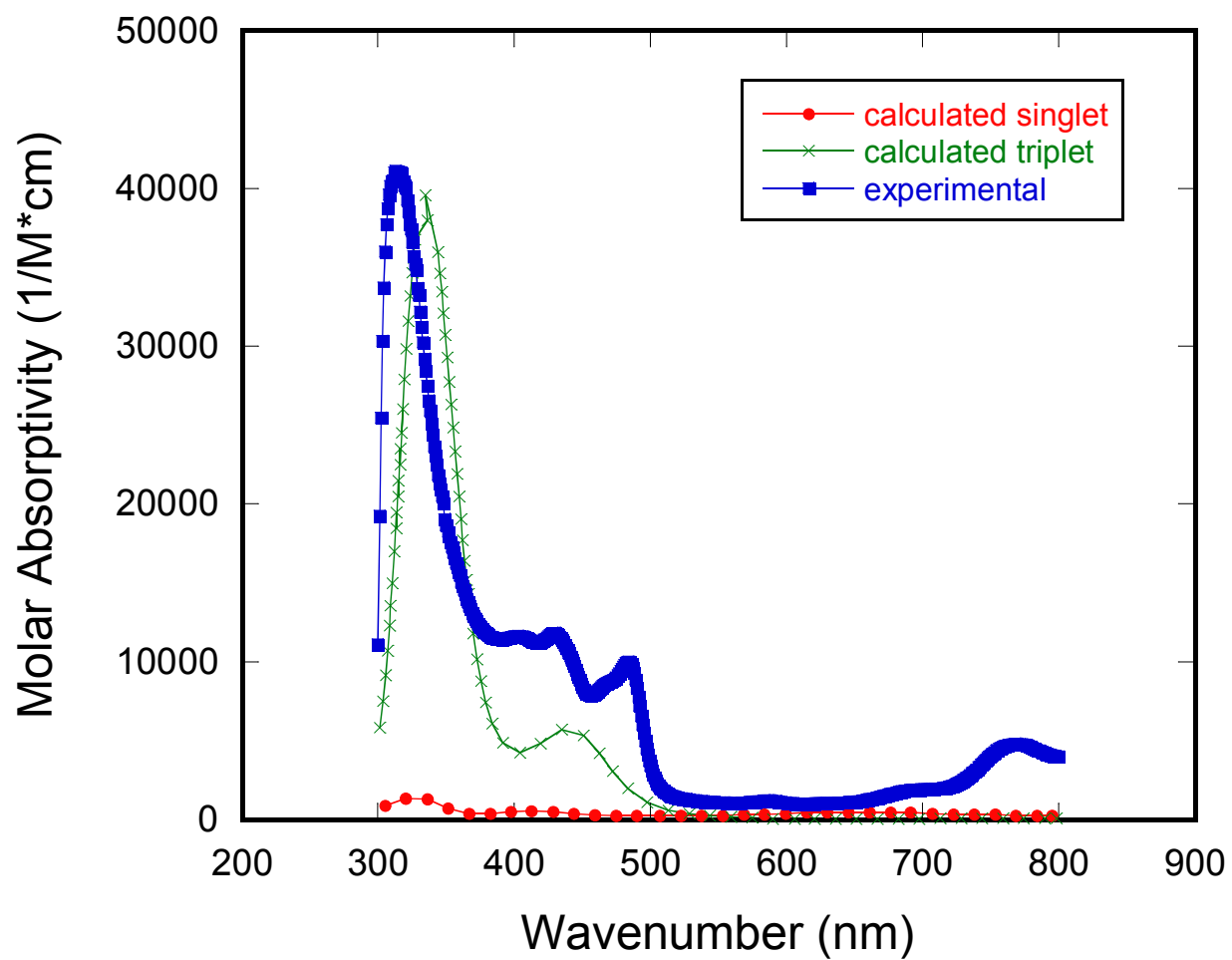


Figure S5. UV-vis spectra for **4** (◆ calculated singlet; × calculated triplet, ■ experimental).

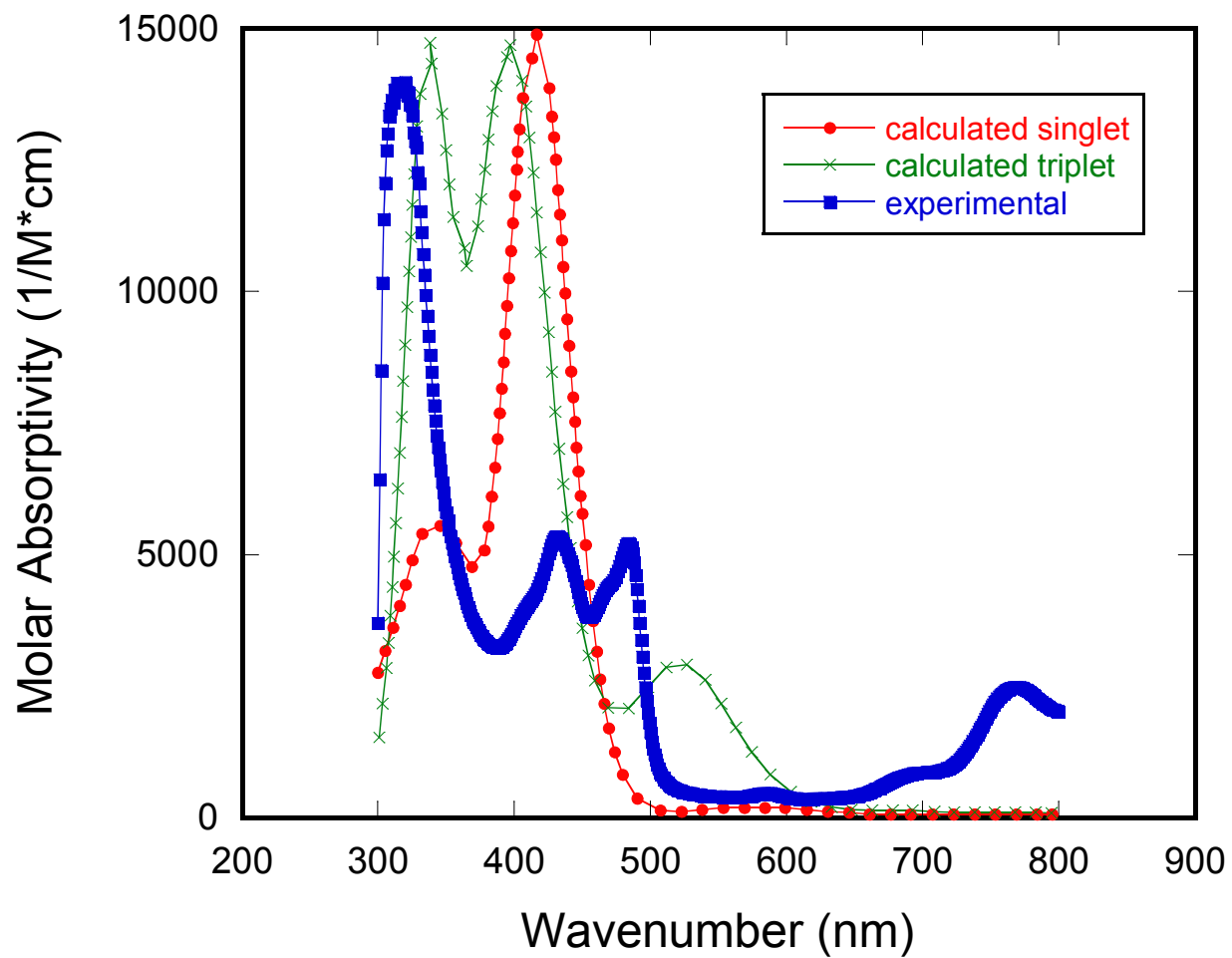


Figure S6. UV-vis spectra for **5** (◆ calculated singlet; × calculated triplet, ■ experimental).

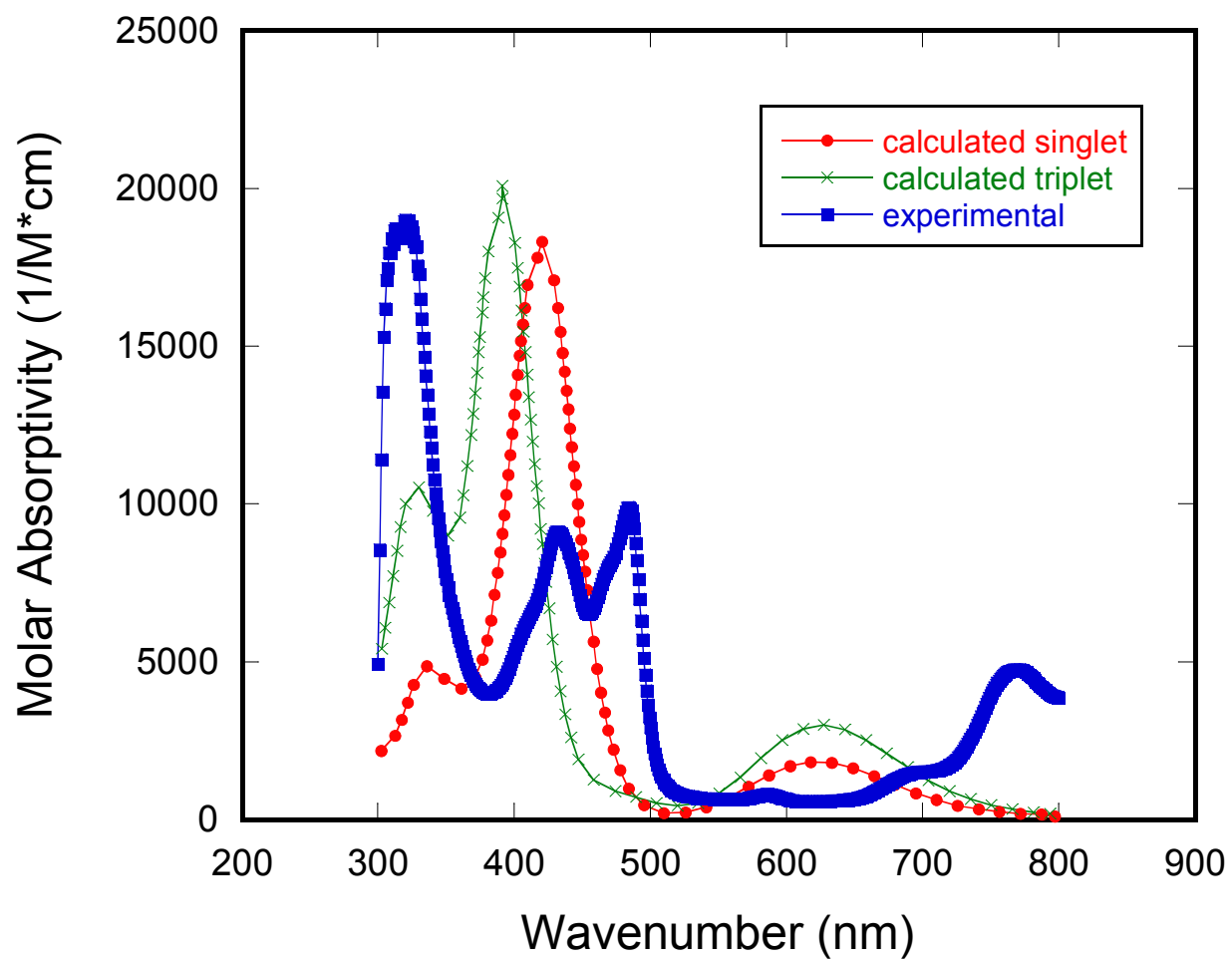


Figure S7. UV-vis spectra for **6** (◆ calculated singlet; × calculated triplet, ■ experimental).

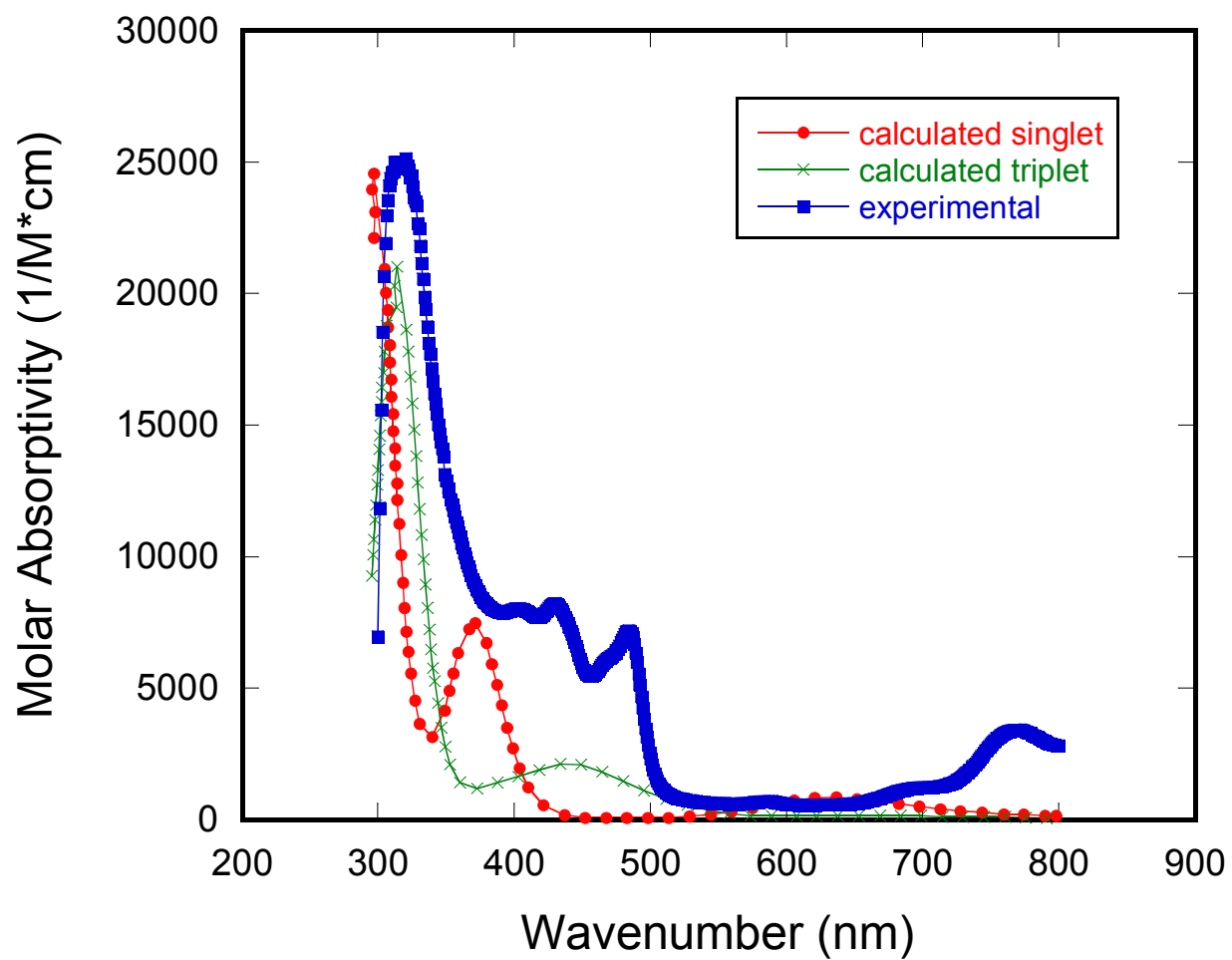


Figure S8. TGA analysis of **1** taken at 25 – 550 °C at a rate of 5 °C per minute under flowing argon.

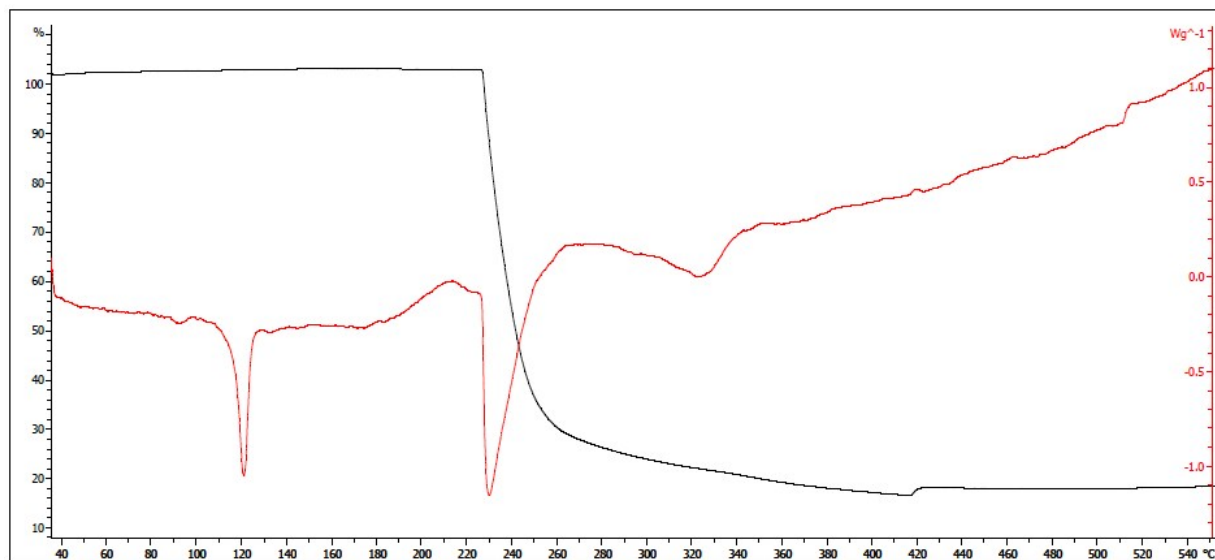


Figure S9. TGA analysis of **6** taken at 25 – 550 °C at a rate of 5 °C per minute under flowing argon.

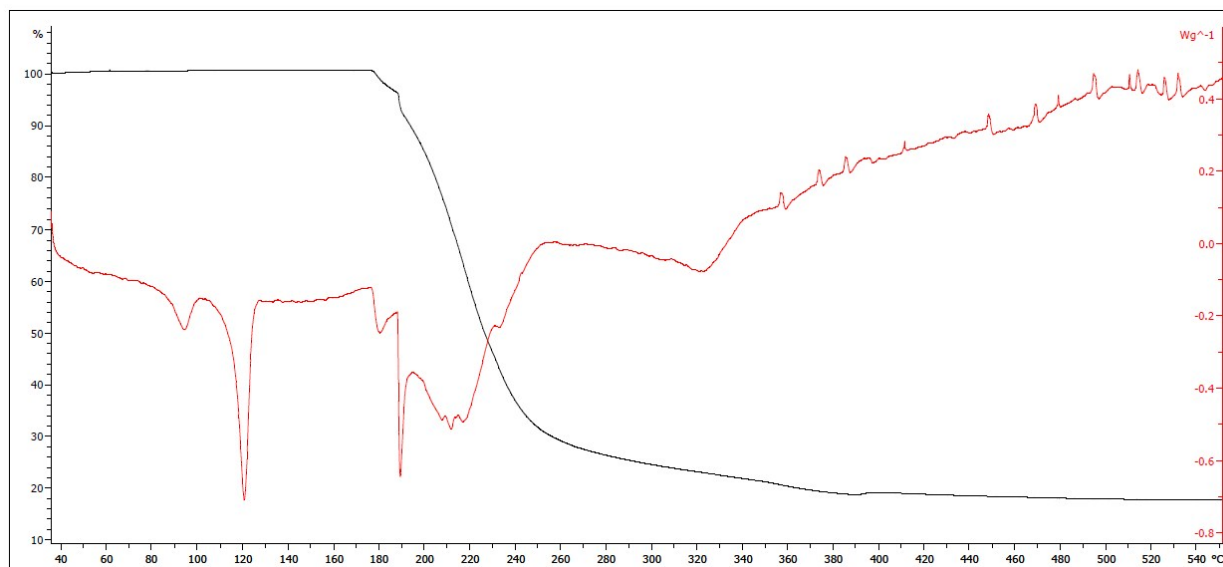


Figure S10. PXRD for the resultant materials from TGA analysis of **1** taken at a range of 10-90° with a scan rate of 0.15 °/sec.

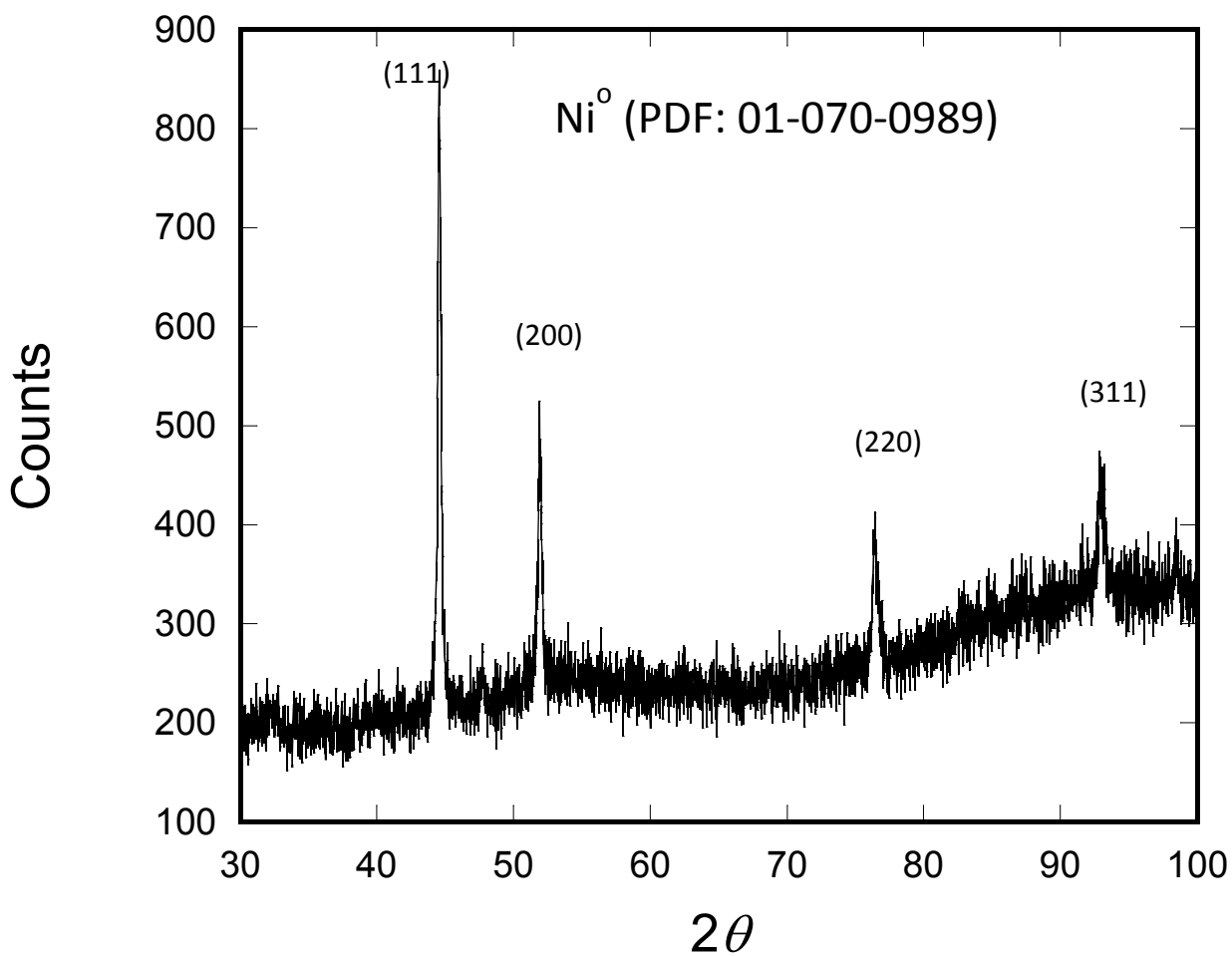


Figure S11. PXRD for the resultant materials from TGA analysis of **6** taken at a range of 10-90° with a scan rate of 0.15 °/sec.

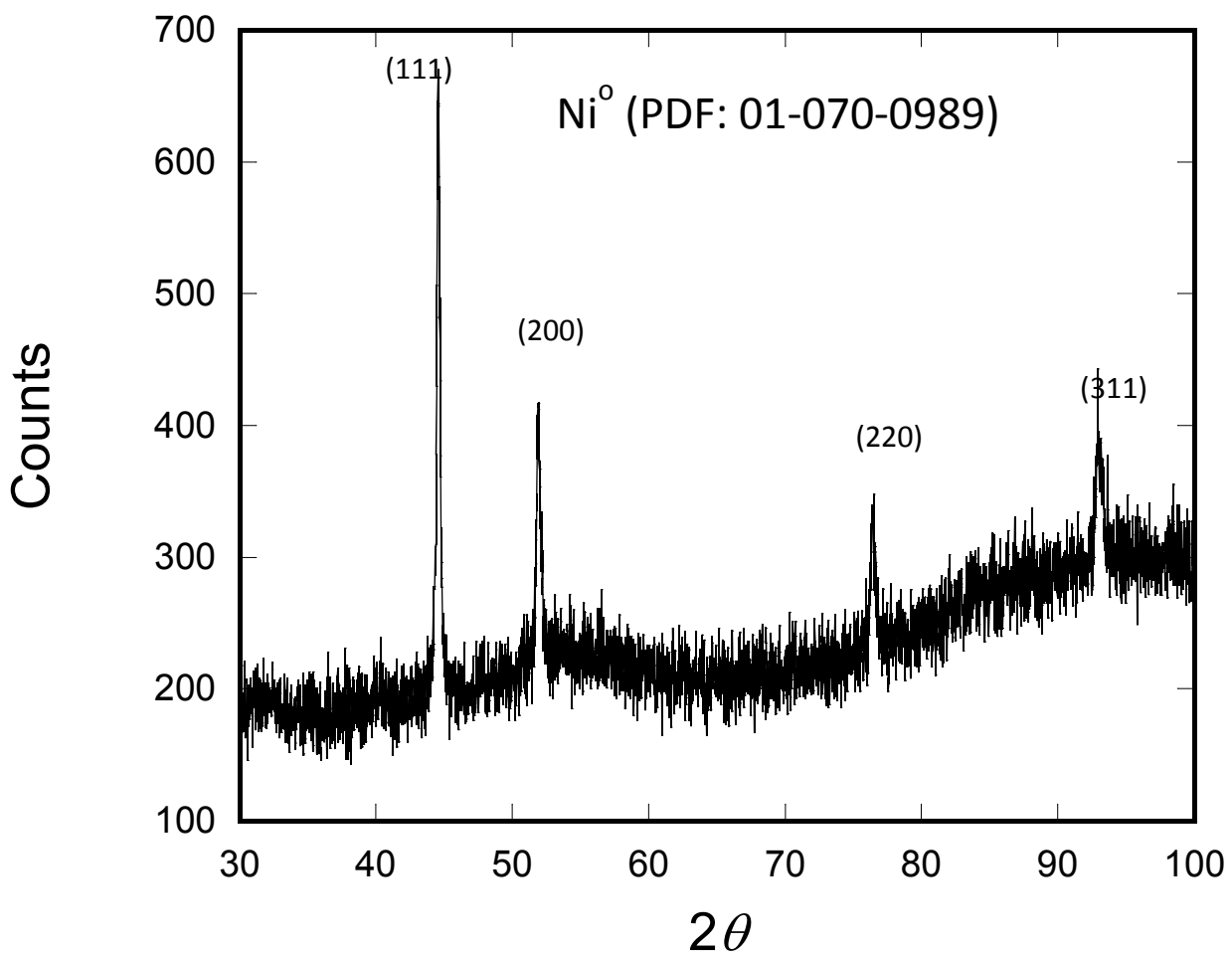


Figure S12. FTIR spectral data (shown from 3800 to 2400 cm^{-1}) for the resultant nanoparticles from the decomposition of **1** and **6**.

